MASS TRANSFER OF NH₃ INTO WATER AT ENVIRONMENTAL CONCENTRATIONS

TAKASHI IBUSUKI†

University of North Carolina, Environmental Sciences and Engineering, Chapel Hill, NC 27514, U.S.A.

and

VINEY P. ANEJA*

Environmental Sciences, Northrop Services Inc., Research Triangle Park, NC 27709, U.S.A.

Abstract—The mass transfer of NH₃ into water at environmental concentrations has been studied in a two-phase flow reactor. The concentration of NH₃ in water ranged from 10^{-6} to 10^{-4} mole $1.^{-1}$ and the temperature was chjanged from 12 to 30°C. At the conditions of this experiment, the overall mass transfer coefficient (K) is more dependent on the hydrodynamics of the gas phase than of the liquid phase. No significant concentration or temperature effects on the value of K have been observed. The mass transport of NH₃ is interpreted in terms of the individual gas phase and liquid phase mass transfer coefficients.

INTRODUCTION

It has been pointed out in past studies on the oxidation mechanism of atmospheric sulfur dioxide in aqueous particles, mists, fogs, and rain (Junge *et al.*, 1958; van den Heuvel *et al.*, 1963; Scott *et al.*, 1967; McKay, 1969; Easter *et al.*, 1974 Hegg *et al.*, 1978) that ammonia may play a significant role in determining the formation rate of sulfate aerosols, despite its very low concentration in the atmosphere. The observed enhancement by NH₃ of the dissolved SO₂ oxidation rates, of the autooxidation, metal ion oxidation and the ozone oxidation is due to its action to raise and maintain a high pH of the water droplet,

The following physical and chemical processes occur to raise and maintain a higher pH through the conversion of NH₃ to NH₄⁺:

(1) Ambient gaseous NH₃(g) dissolves in the water

$$NH_{3(g)} \rightleftharpoons NH_{3(aq)}$$

$$NH_{3(aq)} \rightleftharpoons NH_4^+ + OH^-$$
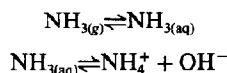
(2) The dissolved NH₃(aq) or OH⁻ reacts with H⁺ or SO₄²⁻/HSO₄⁻ which raises the pH.

As for Step 1, besides the solubility of NH₃ in water, the mass transfer rate of NH₃ into water should be precisely determined since the mass transfer between the gas and liquid phases often becomes a potentially rate controlling step of the gas and liquid phase (heterogeneous) reaction system.

The mass transfer of a gas into water consists of several steps; a diffusion of gas through the gas phase into an interface between the gas and liquid phases, a transport across the interface to the liquid phase boundary and a transfer into the bulk liquid. According to the two-film theory, the main resistance to the mass transfer comes from the gas and liquid phase interfacial films on the assumption that the bulk of each fluid is well mixed (Lewis *et al.* 1924). The overall molecular flux, J, is described by the following equation:

$$J = -K(C_g - HC_l). \tag{1}$$

The gas and liquid phase mass transfer resistances are defined as the reciprocal values of the gas and liquid phase mass transfer coefficients. The value of K is described as follows by using the individual mass transfer coefficients, k_g and k_l,

$$1/K = H/k_l + 1/k_g. \tag{2}$$

In most of the models for estimation of the uptake of gaseous pollutants by water droplets up to the present time (Hales, 1972; Hill *et al.*, 1977; Adamovicz, 1979; Overton, *et al.*, 1979), the following assumptions have been made: the overall mass transfer coefficient, K, is independent of the bulk gas phase concentration of the species and the liquid phase mass transfer resistance, H/k_l, is negligibly small compared to the gas phase one, $1/k_g$, that is $K = k_g$. The value of k_g has been estimated from the semiempirical Frössling equation (Frössling, 1938; and Bird *et al.*, 1960).

Despite abundant research on the mass transfer phenomena of gaseous pollutants such as SO₂, NH₃ and others (Perry *et al.*, 1973), the experimental conditions such as the concentration of the species were very different from real atmospheric conditions. Recently, Rochelle *et al.* (1981) have studied the mass transfer of SO₂ into water at SO₂ partial pressures of 0.0002–0.98 bar. It was revealed that at high SO₂ gas

---

†Present address: National Research Institute for Pollution & Resources, 16–3 Onogawa, Yatabe-cho, Tsukuba–Gun, Ibaraki 305, Japan.

*Author to whom correspondence should be addressed. Present address: General Electric Company, Corporate Research and Development, P.O. Box 8, Schenectady, NY 12301, U.S.A.

phase concentrations the interface mass transfer from gas to liquid is limited by the dissociation of SO_2 in water (liquid phase control). It has been suggested that the mass transfer of SO_2 into water changes from the liquid phase control to the gas phase control at the lower concentrations of SO_2.

With regard to the mass transfer of NH_3 into water, it has been demonstrated from experiments conducted at high concentration of NH_3 that both gas and liquid phases can provide appreciable resistances to the transport (Perry et al., 1973). As well as SO_2, the absorptions of NH_3 into water, however, appeared to be a system of gas absorption accompanied by a fast reversible hydrolysis reaction as indicated by eqn (1). It will be likely therefore that the liquid phase mass transfer coefficient depends on the concentration of NH_3, resulting in the change of the overall mass transfer coefficient K or the change of the ratio of the gas mass transfer resistance to the liquid phase mass transfer resistance.

In the present work we have attempted to determine the rate of transport of NH_3 into water at the same condition as the real atmospheric condition. The concentration of NH_3 in water ranged from 10^{-6} to 10^{-4} mole l^{-1} and the temperature was changed from 12 to 30°C. Together with the overall mass transfer coefficient, the gas phase mass transfer coefficient has been experimentally determined. The liquid phase mass transfer coefficient has been calculated according to eqn (2) showing the additivity of the individual mass transfer coefficients. The enhancement due to the hydrolysis reaction of NH_3 in water is discussed.

A two-phase reactor was designed and fabricated to achieve uniformity of composition in both the gas and liquid phases, with independent control of individual hydrodynamic conditions, film resistances and interfacial area. All the experiments were carried out in flow operation with respect to both gas and liquid to avoid the deviation of the NH_3 concentration due to adsorption on the wall of the reactor and the piping materials.

MASS TRANSFER COEFFICIENTS OF NH₃ INTO WATER AND PHYSICAL PROPERTIES REQUIRED FOR CALCULATION OF THEM

To determine the mass transfer rate of NH_3 into water, NH_3 concentration of both the liquid and gas phases must be precisely measured as can be seen from eqn (1). If the NH_3 gas phase concentration is in the ppb range to simulate atmospheric concentration, the uptake of NH_3 in the liquid phase as the result of the absorption is too low to be measured by conventional analytical methods. Therefore, instead of the absorption rate, the desorption rate was measured on the assumption that the film resistances are the same for absorption and desorption.

In Fig. 1, a material balance on the gas phase of the reactor for the desorption system is presented. The steady state material balance equation for the

thoroughly mixed phase is,

$$\frac{v_g C_{gin}}{V_g} + \frac{aJ}{V_g} = \frac{v_g C_{gout}}{V_g} \qquad (3)$$

$$\text{Input} \qquad\qquad \text{Output}$$

where J is the molecular flux of NH_3 as stated in eqn (1). At the present experimental condition ($C_{gin} = 0$), the overall mass transfer coefficient, K, is given as follows:

$$K = \left(\frac{v_g}{a}\right)\left(\frac{C_g}{HC_l - C_g}\right). \qquad (4)$$

The value of H, Henry's law constant of NH_3, is also required to calculate the overall mass transfer coefficient, K, from this equation. The value of H for NH_3 has been measured or estimated by several investigators (Morgan et al., 1931; McKay, 1971; Edward et al., 1975; Hales, 1979). In this paper, the value of H measured by Hales was selected for calculation of K at 25°C, since it was determined at very low concentrations of NH_3. However, the temperature dependence of H seemed too low by comparison to the other ones as shown in Table 1. A precise value of the heat of solution of NH_3 to water has been determined by using a calorimetric method (Vanderzee et al., 1972). The value of 8448 cal mole^{-1} is considered to be most reliable at the present time and was used to estimate the value of H at different temperatures. Since the plot of $\log H$ vs the reciprocal of the absolute temperature gave a good straight line for each data in Table 1, an empirical equation, $H = H_0 \exp(-8448/RT)$ was used, where R is the gas constant and T is the absolute temperature.

The dissolved ammonia ($NH_{3(aq)}$) rapidly dissociates to produce ammonium (NH_4^+) and hydroxide (OH^-) ions.
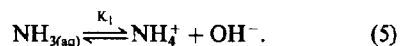
$$NH_{3(aq)} \overset{K_1}{\rightleftharpoons} NH_4^+ + OH^-. \qquad (5)$$

The equilibrium constant, K_1, is defined as follows:

$$K_1 = \frac{[NH_4^+][OH^-]}{[NH_{3(aq)}]}. \qquad (6)$$

Table 1. Henry's law constant of NH_3 to water measured or estimated (mole l^{-1} (gas) mole l^{-1}(liquid) 1×10^4)

TEMP	HALES	McKAY	EDWARD	MORGAN
30°C	6.50		8.31	8.01
25°C	5.42	7.17	6.78	6.67
20°C	4.43		5.42	5.20
15°C	3.65	4.07	3.95	
5°C		2.21		
ΔE*	6.67	9.69	7.56	7.56

*evaluated from a plot of logH vs T^{-1}
(Kcal mole^{-1})

$$C_{gas_{in}} = \text{INLET CONCENTRATION IN THE GAS PHASE (mole/l)}$$
$$C_{gas_{out}} = \text{OUTLET CONCENTRATION IN THE GAS PHASE (mole/l)} = C_{gas}$$
$$C_{liquid_{in}} = \text{INLET CONCENTRATION IN THE LIQUID PHASE (mole/l)}$$
$$C_{liquid_{out}} = \text{OUTLET CONCENTRATION IN THE LIQUID PHASE (mole/l)} = C_{liquid}$$
$$V_{gas} = \text{FLOW RATE IN THE GAS PHASE (l/sec)}$$
$$a = \text{AREA OF INTERFACE (cm}^2)$$
$$\overline{V}_{gas} = \text{VOLUME OF THE GAS PHASE CHAMBER (l)}$$
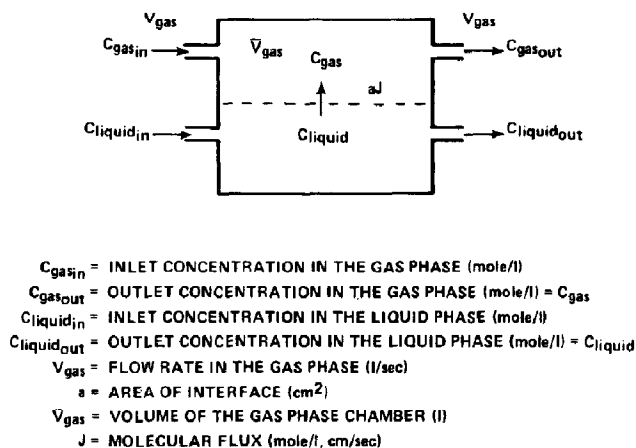$$J = \text{MOLECULAR FLUX (mole/l, cm/sec)}$$

Fig. 1. Material balance on the system gas phase of the two phase reactor for desorption system.

Electrical neutrality requires that the concentration of hydroxide ion, [OH$^-$], is always equal to that of NH$_4^+$, [NH$_4^+$], since there is no other ionic species in this system.

$$[NH_4^+] = [OH^-]. \tag{7}$$

In this experiment, only the concentration of the total nitrogen, C_+ was measured with an ion chromatograph:

$$C_+ = [NH_4^+] + [NH_{3(aq)}] \tag{8}$$

The concentration of the dissolved ammonia, [NH$_{3(aq)}$], which is needed to determine the mass transfer rate of NH$_3$ to water, should therefore be calculated according to the following equation derived from eqns (6)–(8).

$$[NH_{3(aq)}] = \frac{2C_+ + K_1(1 - \sqrt{1 + 4C_+/K_1})}{2}. \tag{9}$$

The other solution containing a positive root has not been chosen, since the value of [NH$_{3(aq)}$] was larger than the value of C_+ if the positive root was chosen (see eqn 8).

The value of K_1 at the temperature ranging from 12 to 30°C was calculated according to the following equation estimated from the literature data (Bates et al., 1950; Emerson et al., 1975).

$$\log K_1 = -3.982 - \frac{230.98}{T}. \tag{10}$$

EXPERIMENTAL

A schematic diagram of the experimental set-up is shown in Fig. 2. The complete apparatus consists of a 2-phase reactor made of Pyrex glass and liquid flow controls systems, and analytical systems. The 2-phase reactor was designed and fabricated similarly to the one in literature (Levenspiel et al., 1974; Aneja, 1975).

The reactor has two variable speed continuous duty motors and agitators with four flat blades for mixing of the gas and liquid phases with the baffles around the reactor wall and bottom for the rapid and complete mixing. An interface plate was constructed of a 0.15 cm thick FEP Teflon sheet and the interface holes were drilled with a quarter inch drill and the size of each hole was measured. The plate was placed between the upper and lower compartments of the reactor and was secured with bolts spaced around the flange. The temperature of the reactor was controlled and maintained constant by circulating temperature-controlled water in the water jacket surrounding the reactor. The temperatures at the inlet and outlet of the gas and liquid and the pressure of the reactor were monitored with thermocouples covered with glass, and thermometers (YSI Co.) and with a pressure gauge, respectively. Only Teflon and Pyrex glass were used for the experimental system to keep the gas and the liquid from contamination and to avoid adsorption of NH$_3$ on the wall or the piping system.

Aqueous solutions of NH$_4$OH in concentrations ranging from 8×10^{-6} to 2×10^{-4} moles l^{-1} were prepared from the reagent grade NH$_4$OH aqueous solution (28–30% NH$_3$) and water. Tap water was passed through an activated carbon and two ion-exchange resin containing tanks to remove organic matter and ionic species. The water was then boiled thoroughly under nitrogen atmosphere to remove dissolved carbon dioxide, since NH$_3$ may react with CO$_2$, resulting in the change in the mass transfer rate of NH$_3$ (Hales, 1979). The solution was stored in a polypropylene tank (ca. 20 liters of volume) under N$_2$ and was introduced to the lower reaction compartment and the fluid was stirred at an agitation rate from ca. 100 to 300 revolution per minute (rpm). The molecular ammonia desorbed from the solution to the gas phase (the upper compartment) and was mixed immediately with nitrogen (an agitation rate of ca. 100–600 rpm and a flow rate of about 750 cm^3 min^{-1}). Research grade cylinder nitrogen was passed through a purification train hav-
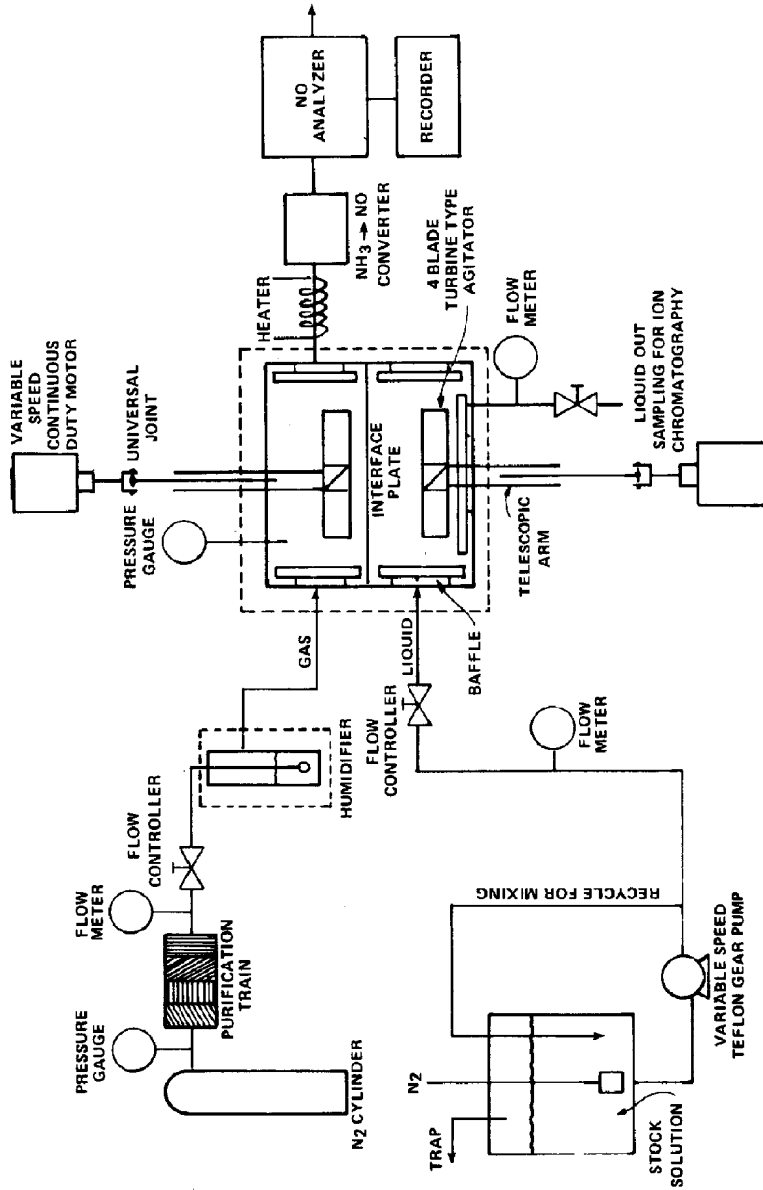
Fig. 2. Block diagram of experimental set up.

ing an Ascarite column for CO_2 removal, a Purafil sieve for NO_x removal, an activated charcoal trap for organics, a Drierite trap for humidity, and a filter for particulate removal, in that order. The purified nitrogen was humidified by passing through a bubbler containing the purified water and was led to the upper compartment of the reactor. The flow rate was strictly controlled by using a mass-flow controller calibrated with a soap-film gas-flow meter prior to use.

Concentration of NH_3 in the gas phase, C_g, was continuously measured and recorded with a NO chemiluminescent analyzer (Monitor Labs Model 8440). A high temperature stainless steel converter (Thermo Electron Co.) was used to oxidize NH_3 to NO (Aneja et al., 1978). The calibration of the NO analyzer and the check of the conversion efficiency of the converter were performed on each run day by using NO standard gas mixtures (Matheson Gas Products) and NH_3 permeation tubes (Metronics Co.) maintained in a thermostatic water bath, respectively. The permeation rates of the NH_3 tubes were periodically checked by weight loss technique.

Concentration of total nitrogen of the solution was determined using an ion chromatograph (Dionex Co.). Calibration standards were prepared from reagent grade ammonium chloride. The concentration of molecular ammonia in the solution, C_l, was calculated by considering the equilibrium between NH_3 and NH_4^+ as discussed before.

Research grade oxygen in cylinder was introduced to the upper compartment of the reactor at a flow rate of $250\ cm^3\ min^{-1}$ and was absorbed by pure deoxygenated water in the lower compartment. A flow rate of water was strictly controlled and was accurately measured by a weighing method. Oxygen concentrations in water at the inlet (C_i) and the outlet (C_o) of the reactor were measured with a dissolved oxygen meter (Yellow Springs Instrument Co., Model 54 ARC). The calibration of the oxygen meter was carried out for each run according to the instruction manual.

RESULTS AND DISCUSSION

Effect of agitation rates in the gas and liquid phases on overall mass transfer coefficient

Desorption rates of NH_3 from water were measured at different agitation rates of both the gas (n_g) and the liquid phases (n_l) at the temperature of 25.2°C. The agitation were independently controlled and changed within the rates of $n_g \sim 600$ rpm and $n_l \sim 300$ rpm to keep a smooth interfacial surface of water. The overall mass transfer coefficient was calculated according to eqn (4). In Figs. 3 and 4, the dependence of K on the agitation rates of the gas phase and of the liquid phase are shown. Both the values of n_g and n_l have been converted to the dimensionless numbers showing the hydrodynamic and physical properties of the reactor. (Re: Reynolds number defined as nDa^2/v where n, Da, and v are the agitation rates of the gas or liquid phase, a diameter of the agitator blade, and the kinematic viscosities of

nitrogen and water, respectively. D: agitation position, distance from interface to agitator blade centerline, and L: height or depth of liquid phase in reactor.) The values of K increased with increasing agitation rates, $(Re)_g(D/L)_g$ and $(Re)_l(D/L)_l$. It can be seen from the relationships that the influence of the gas phase agitation rate is much greater than that of the liquid phase. The magnitude of increase in K corresponding to the 4 fold increase of $(Re)_g(D/L)_g$ was ca. 100%, whereas that for $(Re)_l(D/L)_l$ phase was only ca. 25%. This suggests that the gas phase mass transfer coefficient, k_g, makes a larger contribution to the overall mass transfer of NH_3 to water than the liquid phase coefficient, k_l. The details will be discussed in later sections.

Effect of concentration of NH_3 on overall mass transfer coefficient

As discussed previously, the values of K previously reported have been measured at much higher concentrations than those found in ambient air. Since there is the possibility that the value of K is a function of the NH_3 concentration, the values of K at different concentrations of NH_3 have been systematically measured (Table 2). The concentration of NH_3 was changed from 8×10^{-6} to 1.2×10^{-4} mole l^{-1} and the agitation rates of both phases were at the highest values.

The values of K were plotted against the concentration of NH_3 in the liquid phase, C_l, in Fig. 5. It is observed that the value of K is constant regardless of the large change of C_l. This is more clearly demonstrated from Figure 6, in which the plot of J against the values of $(C_g - HC_l)$ gave a straight line fit passing through the origin. The mean value of K was calculated to be 2.65 cm sec^{-1} with the standard derivation of ± 0.13. This value is not different from the literature ones ($0.6 \sim 2.3$ cm sec^{-1}) which were determined by using the same kind of reactor at much higher concentrations ($C_g \sim 10^{-2}$ atm and $C_l \sim 10^{-2}$ mole l^{-1}) (Godfrey et al., 1973; Levenspiel et al., 1974). It seems reasonable to conclude that the value of K is independent of the NH_3 concentration over the range of concentrations investgated. This conclusion seems much different from that for SO_2 and will be discussed in a later section.

Effect of temperature on overall mass transfer coefficient

To know whether the value of K depends on the temperature or not is considered very important for the modelling of the atmospheric sulfate formation in the presence of NH_3, because of frequent change of meteorological conditions. At the different temperatures of the reactor ranging from 12 to 30°C, the values of K were determined at some concentrations of NH_3 and the highest agitation rates for the gas and liquid phases ($n_g = 576$ rpm and $n_l = 288$ rpm). The values of K are listed in Table 3. (It is confirmed again that the value of K for each temperature run is independent of the concentration of NH_3.) It seems
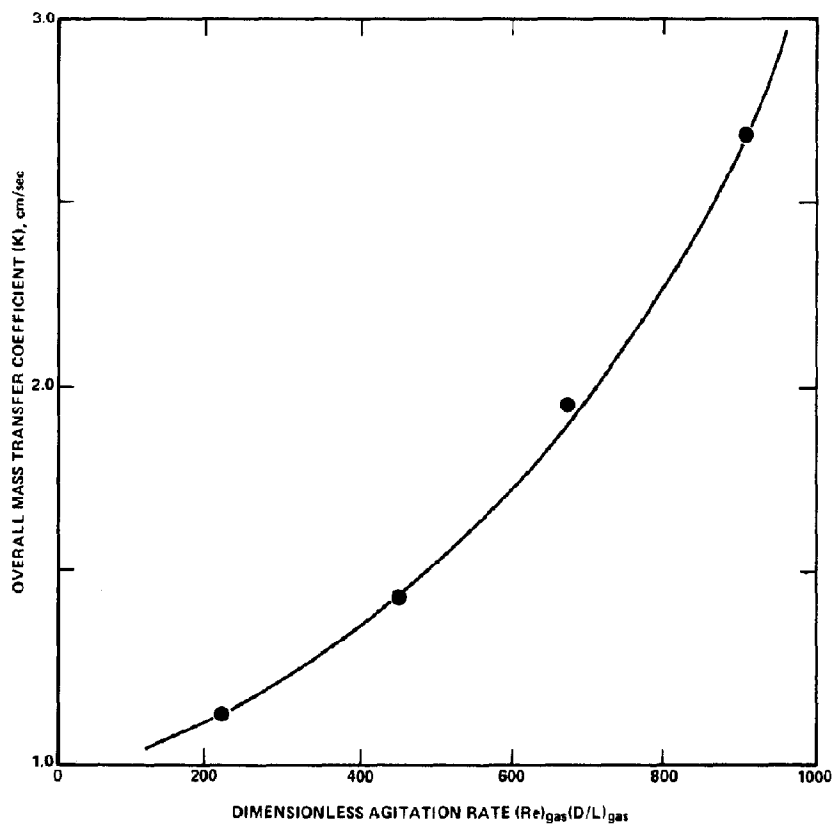
Fig. 3. Change of overall mass transfer coefficient of K with the liquid gas phase agitation rate.

Table 2. Values of K obtained at various NH_3 concentrations*

c_ℓ (mole/l$\times 10^4$)	c_g (mole/l$\times 10^8$)	ν_g/a (cm/sec)	J (mole/l $\cdot$ cm/sec$\times 10^8$)	K (cm/sec)
0.085	0.387	0.566	0.219	2.84
0.105	0.468	0.575	0.269	2.51
0.150	0.678	0.567	0.384	2.73
0.153	0.677	0.564	0.382	2.41
0.180	0.818	0.571	0.467	2.83
0.313	1.42	0.571	0.808	2.81
0.313	1.40	0.571	0.800	2.59
0.342	1.54	0.567	0.873	2.67
0.347	1.55	0.567	0.881	2.55
0.428	1.93	0.564	1.09	2.68
0.831	3.77	0.563	2.12	2.77
0.909	4.06	0.560	2.27	2.52
0.922	4.11	0.560	2.30	2.49
1.27	5.73	0.566	3.24	2.69

*temperature = 25.2°C

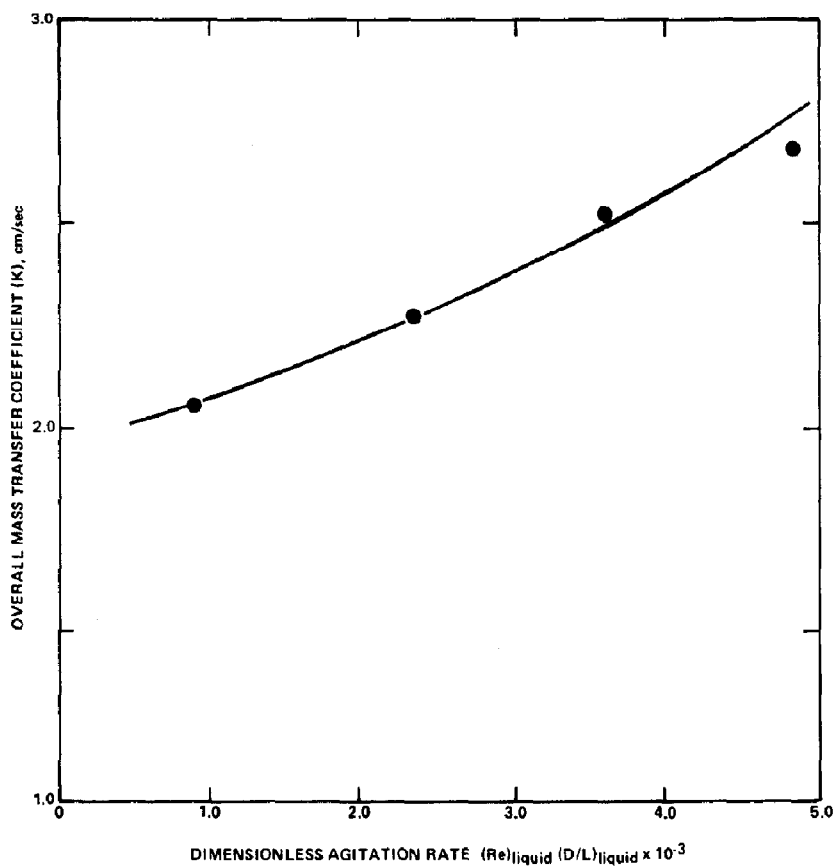stirring rates of n_g = 576 rpm and n_ℓ = 288 rpm

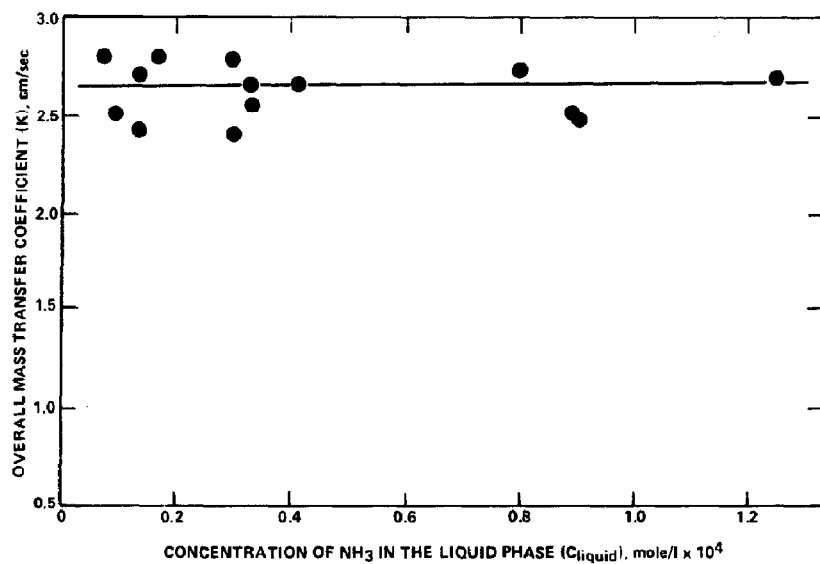Fig. 4. Change of overall mass transfer coefficient of K with the liquid phase agitation rate.

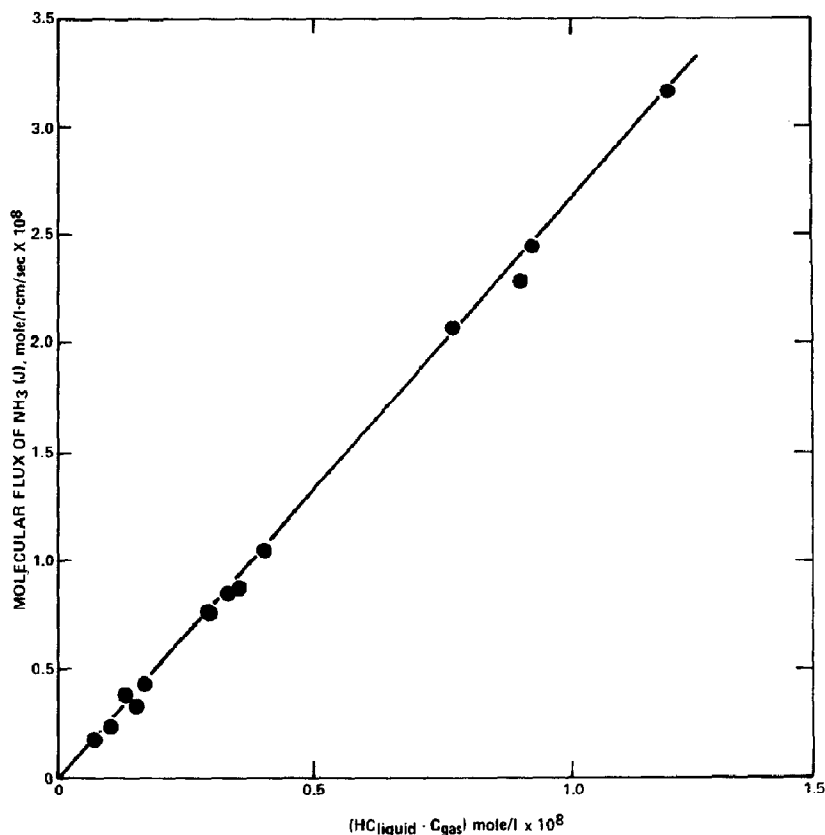Fig. 5. Overall mass transfer coefficient of K at different concentrations of NH$_3$ in the liquid phase (C_l).

Fig. 6. Plot of molecular flux of NH_3 against the value of (HC_f-C_g).

likely that the value of K is constant within the experimental error in the range of experiments. As stated before, K is composed of the mass transfer coefficients of the gas and liquid phases. The results will be discussed in the next section where K is separated into the individual mass transfer coefficients.

Individual mass transfer coefficients of the gas phase and the liquid phase

The gas phase mass transfer coefficient was measured by absorbing NH_3 from NH_3 and N_2 mixture (NH_3 concentration; around 5×10^{-10} mole l^{-1}, prepared by a permeation tube) into sulfuric acid (H_2SO_4) solutions (1×10^{-4} to 2×10^{-3} mole l^{-1}). Both N_2 for the gas mixture and water for the H_2SO_4 solution were prepurified in the same manner as mentioned in the experimental section. Since the dissolved ammonia reacts infinitely fast with respect to mass transfer with a large excess of H_2SO_4 at the gas–liquid interface, the liquid phase mass transfer resistance is considered to be negligible. The concentration of NH_3 at the outlet of the reactor was continuously monitored with the NO analyzer until a constant concentration of NH_3, C_{gout}, was realized. The value of the gas phase mass transfer coefficient,

k_g, was calculated according to the equation (Levenspiel, 1975),

$$k_g = \frac{V_g}{RTa}\left(\frac{C_{gin} - C_{gout}}{C_{gin}}\right) \qquad (11)$$

where V_g is the flow-rate of the N_2/NH_3 mixture and C_{gin} is the concentration of NH_3 at the inlet of the reactor.

The values of k_g measured at the different gas phase agitation rates (144–576 rpm) and the constant liquid phase agitation rate of 288 rpm are summarized in Table 4. It can be seen that the k_g value increases with the increase in the gas phase agitation rate. In Fig. 7, the k_g value was plotted as a function of $\sqrt{Re_g(D/L)_g}$ and $Re_g(D/L)_g$. The plot of k_g vs $\sqrt{Re_g(D/L)_g}$ gave a good straight line as expressed in the following equation,

$$k_g = 0.069\sqrt{Re_g} - 0.394. \qquad (12)$$

The relation that k_g is proportional to the square root of the gas phase Reynolds number is in good accordance with the semiempirical Frössling equation as mentioned in the introduction. It should be noted that the change of the liquid phase agitation rate did

Table 3. Overall mass transfer coefficient at different temperatures,* together with the calculated and observed liquid phase mass transfer coefficient

Temp (°C)	K(cm s^{-1})	1/k$_g$/1/K(%)	k$_\ell^{calc}$	k$_\ell^{obs}$	ϕ***
30.3	2.65	87.1	13.7	6.4	2.1
25.2	2.65	89.4	13.7	5.71	2.4
21.8	2.60	87.5	11.4		
20.0	2.47	83.2	8.03	4.9	1.6
13.1	2.48	83.6	8.27	4.3	1.9
12.0	2.53	85.3	9.41		

* The agitation rates were n$_g$ = 576 rpm and n$_\ell$ = 288 rpm.

** The gas phase mass transfer coefficient was obtained to be 2.97.

*** Enhancement factor = k$_\ell^{calc}$/k$_\ell^{obs}$

Table 4. Gas phase mass transfer coefficient k_g at different gas agitation rates, together with overall mass transfer (n_g) coefficient K and the calculated and observed liquid phase mass transfer coefficient*

n$_g$	k$_g$ (cms^{-1})	K (cms^{-1})	1/k$_g$/1/K(%)	k$_\ell^{calc.}$ (cms^{-1})	k$_\ell^{obs}$ (cms^{-1})	ϕ
576	2.97	2.65	89.4	13.7×10^{-3}		2.4
432	2.33	2.0^	89.7	11.1		2.0
360	2.10	1.91	91.5	11.4	5.71×10^{-3}	2.0
288	1.69	1.56	91.9	11.1		2.0
144	1.35	1.26	93.6	10.7		1.9

*The liquid phase agitation rate is constant (288 rpm) and the temperature was 25.2°C.

not affect the k_g value. It is also found that the effect of the concentration of NH$_3$ in the gas phase or that of temperature on the k_g value was negligible in the experimental range investigated.

The liquid phase mass transfer coefficient, k_l, was calculated from the observed overall mass transfer coefficient, K_1 and k_g according to eqn (2). The calculated k_l value at the constant liquid phase agitation rate (288 rpm) was added to Table 4, it may be reasonable that the k_l value is constant regardless of the change of the gas phase agitation rate. The effect of the liquid phase agitation rate on the k_l value is shown in Fig. 8, in the same manner as done for the k_g. In the agitation rate range of the experiment (54–288 rpm), a similar relationship between k_l and $\sqrt{Re_l(D/L)_l}$ or $Re_l(D/L)_l$ has been observed.

$$k_l = 0.14\sqrt{Re_l} - 5.7. \qquad (13)$$

With regard to the temperature dependence of k_l, the calculated values of k_l are listed in Table 3. Since the temperature dependence of K was not obvious (and k_g was independent of temperature), the temperature dependence of k_l was not clear, but the

declining tendency of k_l with the decrease in temperature was found. This dependence is considered reasonable, since the liquid phase mass transfer coefficient is known to be a function of kinematic viscosity (v) and diffusivity (D_f) which increases with the increase in temperature. On the other hand, the temperature dependence of v and D_f for the gas phase is relatively small, in accordance with the experimental result suggesting temperature independence of k_g.

Relative magnitude of the gas phase mass transfer coefficient and the liquid phase mass transfer coefficient

As can be seen from Table 4, the gas phase mass transfer coefficient, k_g, was about two orders larger than the liquid phase mass transfer coefficient, k_l at the highest mixing condition for both the gas and liquid phases in the experiment. However, because of the high solubility of NH$_3$ into water, the ratio of the liquid phase mass transfer resistance defined as H/k_l to the gas phase mass transfer resistance, $1/k_g$, is not so small as the ratio of k_l/k_g. As listed in the 4th column of Table 4, the liquid phase provides about 10% resistance to the overall mass transport of NH$_3$
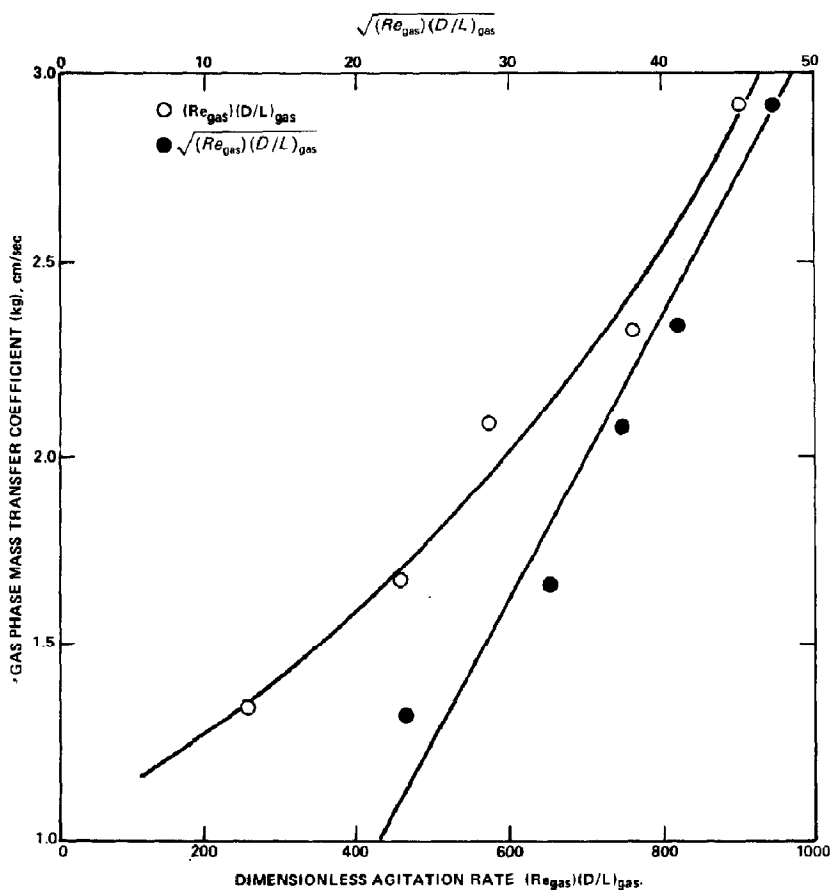
Fig. 7. Correlation of gas phase mass transfer coefficient with dimensionless agitation rate $[Re)_g(D/L)_g]$ and $\sqrt{(Re_g)(D/L)_g}$

to water. The ratio of $1/k_g$ to $1/K$ depended on the mixing condition of the gas and liquid phases. As shown in Table 5, the ratio remarkably decreased from 89 to 70% with the decrease in the liquid phase agitation rate. The change of the ratio with temperature was very small compared to that with the agitation rates as shown in Table 3.

Based on the relationship between k_g or k_l and the related Reynolds numbers (eqns 12 and 13), the gas phase resistance contribution to the overall mass transfer was calculated and is given in Table 6. The following tendencies can be seen from Table 6: (1) the larger the Re_g value, the smaller the gas phase resistance contribution (%); (2) the larger the Re_l value, the larger the gas phase resistance contribution; (3) the gas phase resistance contribution is sensitive to the ratio of $\sqrt{Re_l}/\sqrt{Re_g}$. For example, when the ratio is less than 2, the $1/k_g/1/K$ does not exceed 85% at the

Table 5. Liquid phase mass transfer coefficient k_g at different liquid phase agitation rates,* together with the overall and the gas phase mass transfer coefficient

n_g(rpm)	K (cms^{-1})	k_g (cms^{-1})	$1/k_g/1/K$(%)	$k_g^{calc.}$ (cms^{-1})	k_g^{obs} (cms^{-1})	ϕ
288	2.65		89	13.7×10^{-3}		
216	2.59	2.97	87	11.1	5.1	2.2
126	2.32		78	5.81	3.4	1.7
54	2.07		70	3.74		

*The gas phase agitation rate was constant (576 rpm).

Table 6. The ratio of the gas phase resistance ($1/k_g$) to the overall mass transfer resistance ($1/K$) as a function of the Reynold's numbers in the gas phase $\sqrt{Re_g}$ and the liquid phase ($\sqrt{Re_l}$)

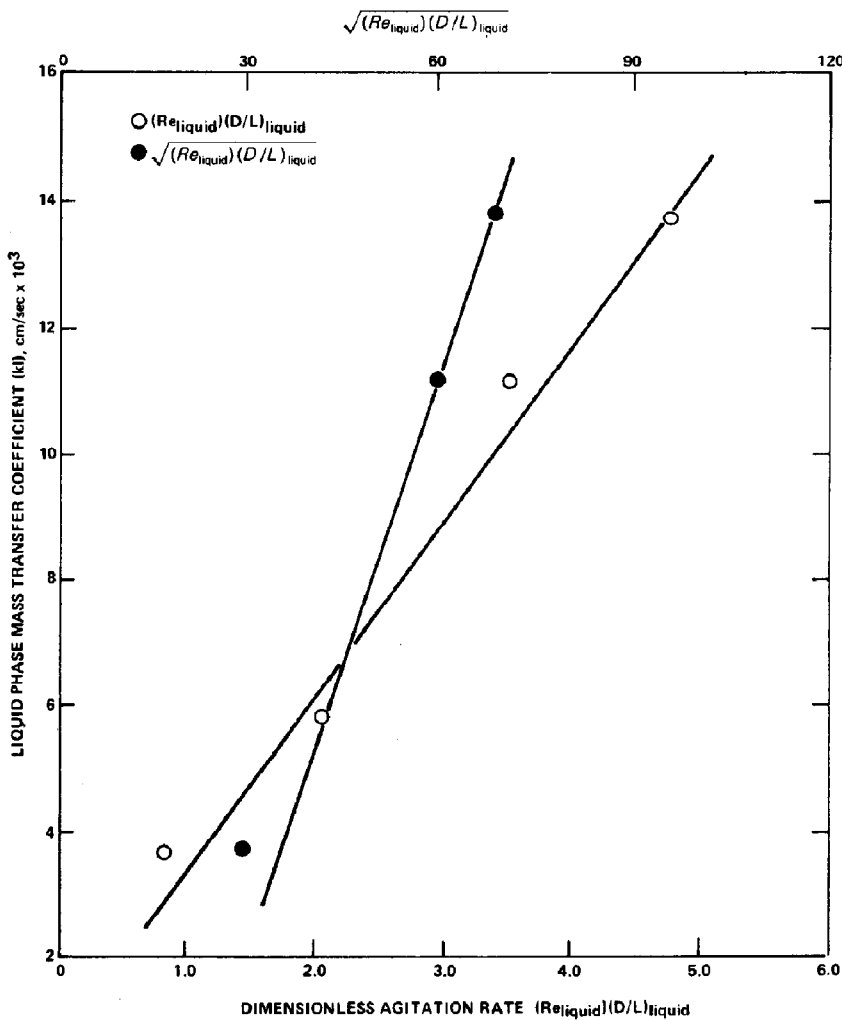| $\sqrt{Re_L}$ \ $\sqrt{Re_g}$	10	20	30	40	50	60	70
50	88.9	70.6	58.7	50.2	43.8	38.9	34.9
75	96.7	89.9	84.0	78.8	74.1	70.1	66.4
100	98.1	93.9	90.1	86.5	83.2	80.2	77.4
125	98.7	95.6	92.8	90.2	87.7	85.3	83.0
150	99.0	96.6	94.4	92.2	90.2	88.2	86.3
175	99.1	97.2	95.4	93.6	91.9	90.2	88.6

Fig. 8. Correlation of liquid phase mass transfer coefficient with dimensionless agitation rate $[(Re)(D/L)_l]$ and $\sqrt{(Re_l)(D/L)_l}$

largest value of Re_g; and (4) at larger values of Re_g, $1/k_g/1/K$ becomes more sensitive to the change of the Re_l. On the other hand at smaller values of Re_l, the contribution becomes more sensitive to the change in Re_g.

Enhancement of mass transfer by NH_3 hydrolysis reaction

It has been mentioned that the hydrolysis reaction of NH_3 may enhance the mass transport by analog with SO_2 mass transport. However, no significant concentration dependence of K was observed. This may imply that the enhancement of mass transfer rate due to the hydrolysis reaction of NH_3 in water is not so large as that found for SO_2-H_2O system (Rochelle *et al.*, 1981).

In order to know the enhancement factor for the liquid phase mass transfer, the physical mass transfer rate of O_2 to water has been measured. Since O_2 is a slightly soluble gas in water and no chemical equilibrium or reaction occurs in water, the mass transfer is controlled only by the liquid phase resistance, that is, the physical mass transfer coefficient can be obtained. Levenspiel *et al.* (1975) have reported that the liquid phase mass transfer coefficient of NH_3 estimated from the measured values of K and k_g is in good agreement with that of O_2. Since their experiment has been conducted at high concentration of NH_3 in both the gas and liquid phases, it will be expected that the NH_3 hydrolysis reaction is highly depressed and can hardly enhance the physical absorption rate of NH_3, resulting in the good agreement of the mass transfer coefficient of NH_3 with that of O_2.

The values of k_l determined at different mixing conditions and temperatures were added to Tables 3–5. It can be seen from Tables 3–5 that the liquid phase mass transfer coefficient k_l^{obs} depends on the liquid phase agitation rate but is not dependent on the gas phase agitation rate. The obvious temperature dependence was also shown in Table 3.

By comparing the observed liquid phase mass transfer coefficient k_l^{obs} for O_2 or NH_3 with the calculated one for NH_3 with respect to each Table, the enhancement factor ϕ was determined to be about 2. This value is very small by comparison to that reported for SO_2-water system.

According to the film theory, the enhancement factor, ϕ, due to the hydrolysis reaction of NH_3 (or SO_2) in pure water can be approximated as follows (Rochelle *et al.*, 1981; Hikita *et al.*, 1978):

$$\phi = 1 + \sqrt{\frac{D_f \overline{NH_4^+}}{D_f NH_3}} \cdot \frac{\sqrt{K_1}}{\sqrt{C_{l_i}} + \sqrt{C_l}}$$

where $D_f NH_4^+$ or D_{OH^-} and $D_f NH_3$ represent the diffusivities of species NH_4^+ or OH^- and dissolved NH_3: C_{l_i} and C_l, the concentrations of the dissolved NH_3 at gas–liquid interface and liquid bulk, respectively.

The $D_f NH_3$ value in pure water was taken as

$2.5 \times 10^{-5}\,\text{cm}^2/\text{sec}$ at $25°C$ (Godfrey, 1973). The effective diffusivity of NH_4^+ ($=OH^-$) was estimated to be $2.86 \times 10^{-5}\,\text{cm}^2/\text{sec}$ at $25°C$ from the Nernst equation (Robinson *et al.*, 1959) using the values of the ionic conductance for the species reported in the literature (Weast, 1975). The C_{l_i} value was calculated from the observed K and k_g values and the Henry's law constant H. The value of K_1 was calculated according to eqn (10). The enhancement factor ranging from 1.3 to 2.0 was estimated from the data given in Table 2. It is clear that the value is in good agreement with the observed values listed in Tables 3–5. The main reason the small ϕ value was obtained for the NH_3- water system is thought to be the higher solubility of NH_3- and the small value of the equilibrium constant, K_1. (The K_1 value for SO_2-water system is about three orders larger than that for the NH_3-water system.)

CONCLUSIONS

Because of the significant role of NH_3 in determining the formation rate of sulfate aerosols, the mass transfer of NH_3 into water at environmental concentrations has been closely studied.

At the conditions of this experiment, the overall mass transfer coefficient (K) is more dependent on the hydrodynamics of the gas phase than of the liquid phase. No significant concentration or temperature effects on the value of K have been found. The results concerning K were well correlated with the individual mass transfer coefficients of the gas phase (k_g) and the liquid phase (k_l). The k_g value was about two orders greater than the k_l value; because of the high solubility of NH_3 in water the liquid phase provides about 10% resistance (not negligible) to the transport. The small enhancement of the liquid phase mass transfer due to the hydrolysis reaction of NH_3 has been confirmed, coinciding with the concentration independence of the overall mass transfer rate.

This study is the first attempt to elucidate the mass transfer phenomena of atmospheric gaseous pollutants at realistic atmospheric conditions. The results supported some of the theoretical or semiempirical assumptions for estimating the mass transfer coefficient. measurements of mass transfer rates of other atmospheric constituents or pollutants such as SO_2, NO_x or CO_2 will be required in this connection. Moreover, measurements of the mass transfer rate of the species in complex systems where various kinds of species coexist may be of importance, despite the difficulty of the measurements, since it is likely that the mass transfer rate will be affected due to chemical reactions among the species and the changing pH value of the droplet.

NOTATION

a area of interface, cm^2

C_g bulk concentration of NH_3 in the gas phase, $mole\,l^{-1}$

C_l bulk concentration of NH_3 in the liquid phase, $mole\,l^{-1}$

D agitator position, cm

Da a diameter of the agitator blade, cm

D_f diffusion constant, cm^2/sec

H Henry's law constant, dimensionless (gas/liquid)

J molecular flux, $mole\, l^{-1}\, cm\, sec^{-1}$

K overall mass transfer coefficient, $cm\, sec^{-1}$

k_g gas phase transfer coefficient, $cm\, sec^{-1}$

k_l liquid phase transfer coefficient, $cm\, sec^{-1}$

K_1 equilibrium constant between NH_3 and NH_4^+, $mole\, l^{-1}$

L height or depth of liquid phase in reactor, cm

n_g agitation rate of the gas phase, $rev\, min^{-1}$

n_l agitation rate of the liquid phase, $rev\, min^{-1}$

R ideal gas law constant, $1.982\, cal\, °K^{-1}$.

T temperature, $°K$

v_g flow rate in the gas phase, $l\, sec^{-1}$

V_g volume of the gas phase compartment, l

Re_g gas phase Reynolds number, dimensionless, $(n_g D_a^2)/v$

Re_l liquid phase Reynolds number, dimensionless, $(n_l D_a^2)/v$

v kinematic viscosity, $cm^2\, sec^{-1}$

ϕ mass transfer enhancement factor

Subscript

in   concentration at the inlet of the reactor, $mole\, l^{-1}$

out   concentration at the outlet of the reactor, $mole\, l^{-1}$

i concentration at gas–liquid interface, $mole\, l^{-1}$

REFERENCES

Adamowicz R. F., *Atmos. Environment* 1979 **13** 105.

Aneja V. P., *Characterization of sources of biogenic atmospheric sulfur compounds*, p. 144. M.S. Thesis, Department of Chemical Engineering, North Carolina State University, Raleigh. 1975.

Aneja V. P., Stahel E. P., Rogers H. H., Witherspoon A. M. and Heck W. W., *Anal. Chem.* 1978 **50** 1705.

Bates R. G. and Pinching G. D. *J. Am. Chem. Soc.* 1950 **72** 1393.

Bird R. B., Stewart W. E. and Lightfoot E. N., *Transport Phenomena*, p. 336. Wiley, New York 1960.

Easter R. C. and Hobbs P. V., *J. Atmos. Sci.* 1974 **31** 1586.

Edward T. J., Newman J. and Praisnitz J. M., *Am. Ind. Chem. Engng. J.* 1975 **21** 248.

Emerson K., Russo R. C., Lund R. E. and Thurston R. V., *J. Fish Res. Bd Can.* 1975 **32** 2379.

Frossling, N. *Beitr. Geophys.* 1938 **52** 170.

Godfrey, J. H. Ph.D. Thesis. Oregon State University, Corvallis 1973.

Hales J. M. *Atmos. Environment* 1972 **6** 635.

Hales J. M. and Drewes R. D., *Atmos. Environment* 1979 **13** 1133.

Hegg D. A. and Hobbs P. V., *Atmos. Environment* 1978 **12** 241.

Hikita H., Asai S. and Nose H., *A.I.Ch.E.J.* 1978 **24**, 147.

Hill F. B. and Adamowicz R. F., *Atmos. Environment* 1977 **11** 917.

Junge C. E. and Ryan T. G., *Q.J.R. Met Soc.* 1958 **84** 46.

Levenspiel O. and Godfrey J. H., *Chem. Engng Sci.* 1974 **29** 1723.

Lewis W. K. and Whitman W. G., *Ind. Engng Chem.* 1924 **16** 1215.

McKay H. A. C., *Chem. Ind.* 1969 1162.

McKay H. A. C., *Atmos. Environment* 1971 **5** 7.

Morgan O. M. and Maass O., *Can. J. Res.* 1931 **5** 162.

Overton J. H. Jr., Aneja V. P. and Durham J. L., *Atmos. Environment* 1979 **13** 335.

Perry R. H. and Chilton C. H., *Chemical Engineer's Handbook*, 5th Edn, p. 18. McGraw-Hill, New York 1973.

Robinson R. A. and Stokes R. H., *Electrolyte Solutions*, 2nd Edn, p. 288. Butterworths, London 1959.

Rochelle G. T. and Chang C. S., *A.I.Ch.E.J.* 1981 **27** 292.

Scott W. D. and Hobbs P. V., *J. Atmos. Sci.* 1967 **24** 54.

Tamir A. and Merchuk J. C., *Chem. Engng Sci.* 1978 **33** 1371.

Van den Heuvel A. P. and Mason B. J., *Q.J.R. Met. Soc.* 1963 **89** 271.

Vanderzee C. E. and King D. L., The Enthalpies of Solution and Formation of Ammonia. *J. Chem. Thermodynamics* 1972 **4** 675.

Weast R. C. *Handbook of Chemistry and Physics*, 5th Edn, D–132. CRC Press, Cleveland, Ohio 1975.